Last Name Invacanza **Given Name** Allegra **ID Number** 20190719

Question n. 1

Write the expression of the sensitivity of a mode-split gyroscope in terms of output voltage per unit angular rate, and identify the three fundamental transduction sub-mechanisms forming the sensitivity. For each of these three sub-mechanisms, comment in details on the sources of instability vs temperature and of variability from part to part, as well as on the strategy that one can adopt to mitigate these effects.

The sensitivity of a mode-split gyroscope can be written as $S_v = \frac{\partial y}{\partial \Omega} \cdot \frac{\partial C}{\partial y} \cdot \frac{\partial V}{\partial C}$, highlighting the different transduction mechanisms.

As for the first term, we know that for a mode-split gyroscope, the expression for the displacement sensitivity is $S_y = \frac{\partial y}{\partial \Omega} = \frac{x_d}{\omega_s - \omega_d} = \frac{x_d}{\omega_s\left(1-\frac{\omega_d}{\omega_s}\right)}$.

At the denominator, due to the thermal drift of the Young modulus of silicon of -60 ppm/K, ω_s drifts by -30 ppm/K. The ratio of the two angular frequencies instead remains constant. Nonetheless, the main source of variability in temperature is given by the displacement x_d. The complete expression for the displacement is the following:

$$x_d = V_d \eta_{da} \frac{Q_d}{k_d}$$

x_d is proportional to Q_d, which is a parameter that exhibits a strong dependence on temperature. We can quantify it starting from the known relationship $Q = \frac{\alpha}{\sqrt{T}}$. Therefore, we can write:

$$\frac{dQ}{Q} = -\frac{1}{2}\frac{dT}{T} \Rightarrow \frac{\frac{dQ}{Q}}{dT} = -\frac{1}{2T} = -\frac{1}{2 \cdot 300K} = -1.6 \cdot 10^{-3}\frac{1}{K} = -1600\frac{ppm}{K}$$

where we have linearized around room temperature.

On top of this, x_d suffers from a +30 ppm/K dependence due to the inverse proportionality with k_d. Overall, recalling that if $S \propto a^k \cdot b^l \cdot c^m \Rightarrow \frac{dS}{S} = k\frac{da}{a} + l\frac{db}{b} + m\frac{dc}{c}$, we can write:

$$S_y \propto \frac{1}{\omega_s} \cdot Q_d \cdot \frac{1}{k_d} \Rightarrow \frac{\frac{dS_y}{S_y}}{dT} = -\frac{\frac{d\omega}{\omega}}{dT} + \frac{\frac{dQ}{Q}}{dT} - \frac{\frac{dk}{k}}{dT} = (+30 - 1600 + 60)\frac{ppm}{K} = -1570\frac{ppm}{K}$$

This strong instability can be dealt with at system-level by making use of an AGC loop that, by acting on the driving amplitude, is able to reduce the change in displacement by a factor of $1 + G_{loop,agc}$ (which can be 10 or 20, in a realistic case).

In terms of part-to-part variation, neglecting second-order effects, the main source of part-to-part variability is the spread in the etching process. This gives an uncertainty in the width of springs and gaps whose standard deviation can be few tens of nanometers. If one wants to lower this spread, he can design wider (and longer) springs and wider gaps (at the expense of a larger area occupation and/or a decrease in the overall sensitivity). Also, the height of the process can change from part-to-part (≈1 µm, 5 % for a 20 µm thick process), but since k, m, η_{da} are proportional to it, this spread does not affect the displacement sensitivity.

The second mechanism of transduction is the capacitive read-out $\partial C/\partial y$. Assuming a parallel-plate read-out (which maximizes the sensitivity for a given area), this term can be written as:

$$\frac{\partial C}{\partial y} = \frac{2N_{PP}L_{PP}h}{g_{PP}^2}$$

In this case, we can identify no significant temperature dependence. But the same considerations discussed above on the etching and height spread apply here. Specifically, $\partial C/\partial y$ is affected strongly by the gap, but also by the process height, unlike $\partial y/\partial \Omega$. Overall, thus, a process height increase or a gap decrease will increase the sensitivity from part to part.

Finally, the third transduction mechanism is the charge amplifier transduction for a rotor biased with a DC voltage V_{DC}:

$$\frac{\partial V}{\partial C} = \frac{V_{DC}}{C_f}$$

This term is very stable in temperature. To address the variability of V_{DC} from part to part instead, we should know something more regarding the circuits (called charge pumps) that are able to provide the high voltage to the MEMS rotor. We neglect this term in this discussion, as this is usually very stable.

As for the capacitance C_f, a typical part-to-part spread for an integrated capacitance in the order of few hundreds fF to few pF (typical values for MEMS circuits) is about $\pm$20% maximum.

Note that all the part-to-part sources of variability can be combined altogether and can be compensated to a large extent in the final product, using a digital compensation after an initial calibration at the rate table.

Last Name Invacanza **Given Name** Allegra **ID Number** 20190719

Question n. 2

Consider the MEMS accelerometer represented in the figure, to sense accelerations along the x-direction. Its parameters are reported in the table below. In particular, we note that it is characterized by ultra-narrow gaps, and by a stiffness in the y-axis direction much larger than for the x-axis sensing direction, as expected.

Parameter	Symbol	Value
Gap	g	0.25 µm
Comb overlap at rest	L_{ov}	10 µm
Process height	h	30 µm
N_{L1} N_{L3} N_{R1} N_{R3}	N_S	32
N_{L2} N_{R2}	N_{test}	11
Stiffness in the x direction	k_x	5 N/m
Stiffness in the y direction	k_y	987 N/m
Q factor in the x direction	Q_x	2
Mass	m	9 nkg
Full-Scale Range	FSR	±4 $\tilde{g}$
Amplifier bias voltage	V_{dd}	±3 V
Feedback Capacitance	C_f	150 fF

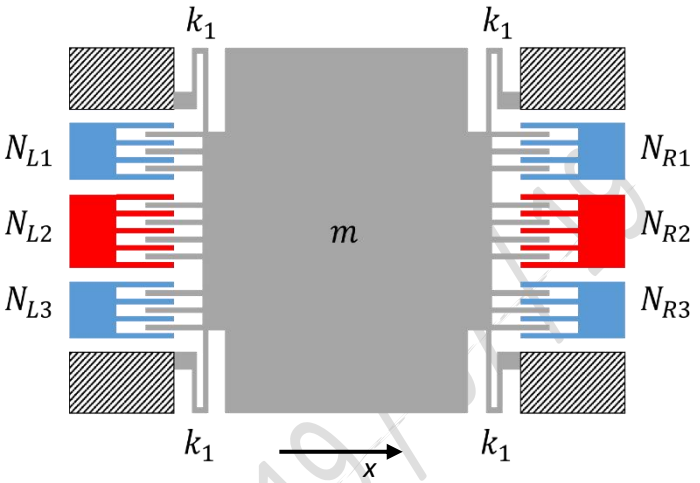

(i) During a self-test calibration procedure, a voltage *V(t)* that slowly ramps from 0 V to 5 V is applied to all left electrodes (N_{L1}, N_{L2}, N_{L3}). Draw the capacitance variation measured at the combined right ports (N_{R1}, N_{R2}, N_{R3}) as a function of the applied voltage (indicate in particular the maximum capacitance variation in the graph). The rotor is grounded as shown.

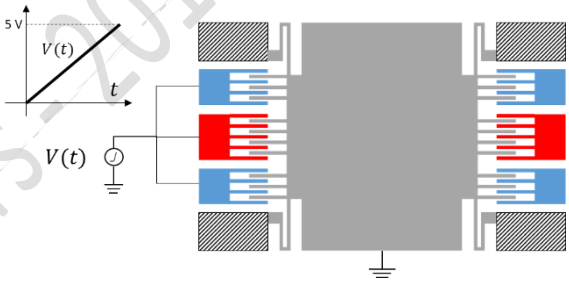

(ii) In a second calibration procedure, a voltage ramp $V_1(t)$ from 0 V to 5 V, summed to a DC value of 5 V, is applied to electrode N_{L2}; a voltage ramp $V_2(t)$ from 0 V to -5 V, summed to a 5 V DC value, is applied to electrode N_{R2}. Draw the differential capacitance variation between the remaining right ports (N_{R1}, N_{R3}) and left ports (N_{L1}, N_{L3}) as a function of the differential applied voltage. In particular, write the maximum capacitive change.

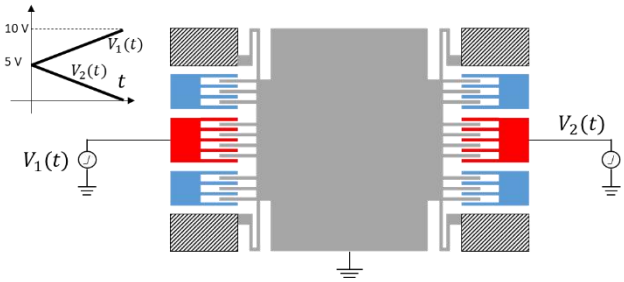

(iii) Assume that the sensor is now connected to its charge amplifier circuit, as shown (all left ports at $+V_{dd}$, all right ports at $-V_{dd}$). Find the gain needed at the second stage to cope with the target FSR, assuming that the stators are biased at the same voltages of the supply, as indicated (with $\pm V_{dd}$ = ±3 V).

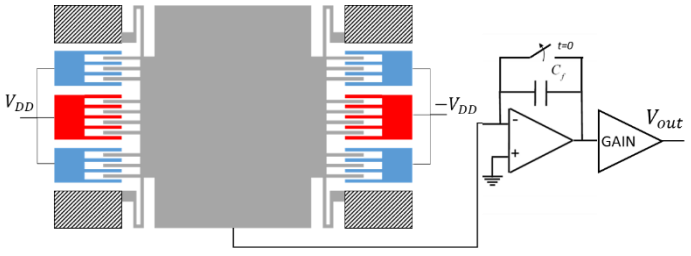

(iv) Calculate the new value of the sensitivity if the stators are now biased to a dedicated voltage, now doubled to $\pm V_{dd}$ = ±6 V.

Physical Constants

k_b = 1.38 10^{-23} J/K;
ε_0 = 8.85 10^{-12} F/m;
T = 300 K;

(i)

This configuration corresponds to a single-ended quasi stationary drive using comb fingers. In this case the electrostatic force is represented by the following expression:

$$F_{elec}(t) = -\frac{V(t)^2}{2}\frac{dC_D}{dx} = \frac{V(t)^2}{2}\frac{d(C_{L1+L2+L3})}{dx} = -\frac{V(t)^2}{2}\frac{2\epsilon_0(N_{L1}+N_{L2}+N_{L3})h}{g}$$

As the electrostatic force is attractive, the negative displacement will induce a negative capacitance variation at the ports used for sensing, whose capacitance thus changes by :

$$\Delta C_{R1+R2+R3}(V) = \frac{\mathrm{d}C_{R1+R2+R3}}{dx}\frac{F_{elec}(t)}{k} = \frac{2\epsilon_0(N_{R1}+N_{R2}+N_{R3})h}{g}\frac{F_{elec}(t)}{k} =$$

$$= -\left(\frac{(2\epsilon_0(N_{L1}+N_{L2}+N_{L3})h}{g}\right)^2\frac{1}{k}\frac{V(t)^2}{2}$$

The graph of the capacitance variation is reported below. The maximum value can be calculated for the maximum drive voltage of 5 V and corresponds to about -63.5 fF.

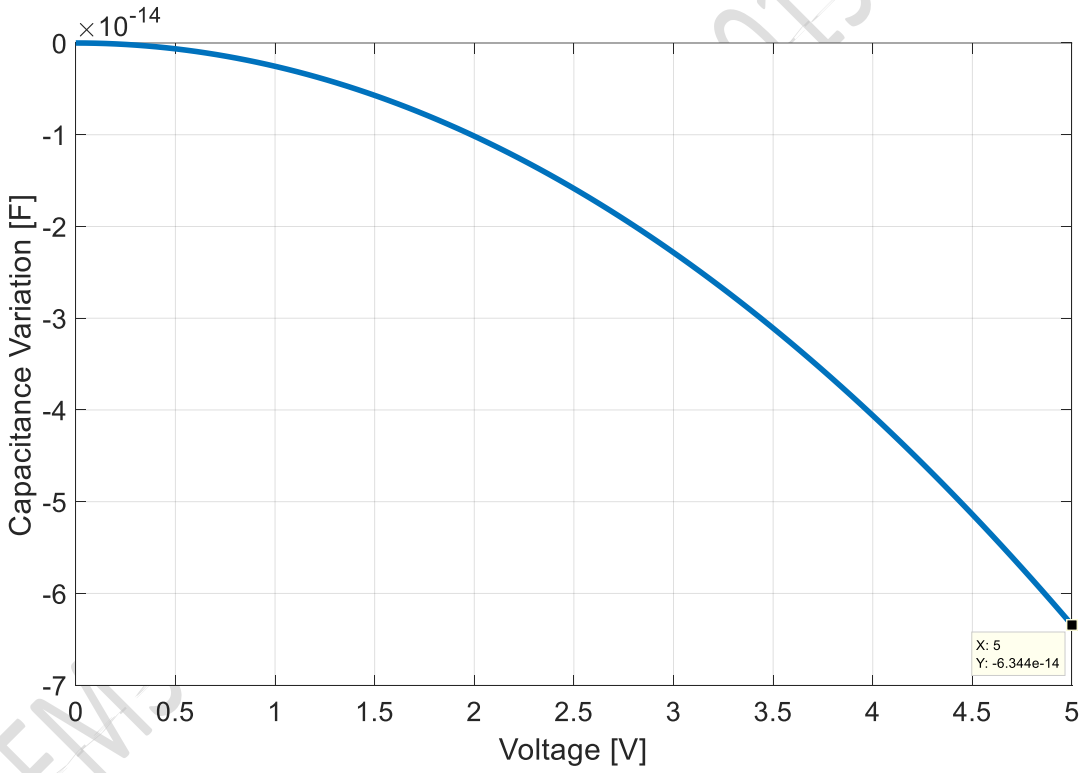

(ii)

This second situation correponds to the case of a push-pull drive through comb fingers. Taking into account that the two stators apply opposite forces, the expression of the electrostatic force becomes:

$$F_{elec}(t) = -\frac{\left(V_{DC}+V(t)\right)^2}{2}\frac{dC_{DL}}{dx} + \frac{\left(V_{DC}-V(t)\right)^2}{2}\frac{dC_{DR}}{dx} =$$

$$= -\frac{V_{DC}^2+V(t)^2+2V_{DC}V(t)}{2}\frac{2\epsilon_0 N_{L2}h}{g} + \frac{V_{DC}^2+V(t)^2-2V_{DC}V(t)}{2}\frac{2\epsilon_0 N_{R2}h}{g} =$$

$$= -\frac{4V_{DC}V(t)}{2}\frac{2\epsilon_0 N_{L2}h}{g}$$

In agreement with push-pull driving, the force is linear with the applied voltage. As a consequence, the capacitance variation is linear too, and is given by:

$$\Delta C_{R1+R3}(V) - \Delta C_{L1+L3}(V) = \frac{\mathrm{d}C_{R1+R3}}{dx}\frac{F_{elec}(t)}{k} - \frac{\mathrm{d}C_{L1+L3}}{dx}\frac{F_{elec}(t)}{k} = 2\frac{\mathrm{d}C_{L1+L3}}{dx}\frac{F_{elec}(t)}{k} =$$

$$= -\left(\frac{2\epsilon_0 h}{g}\right)^2 N_{L2}(N_{L1}+N_{L3})\,\frac{4V_{DC}V(t)}{k}$$

The requested graph of the capacitance variation is reported below. The maximum value can be calculated for the maximum drive voltage of 5 V and corresponds again to -63.5 fF. Note however the perfect linearity of this characterization procedure.

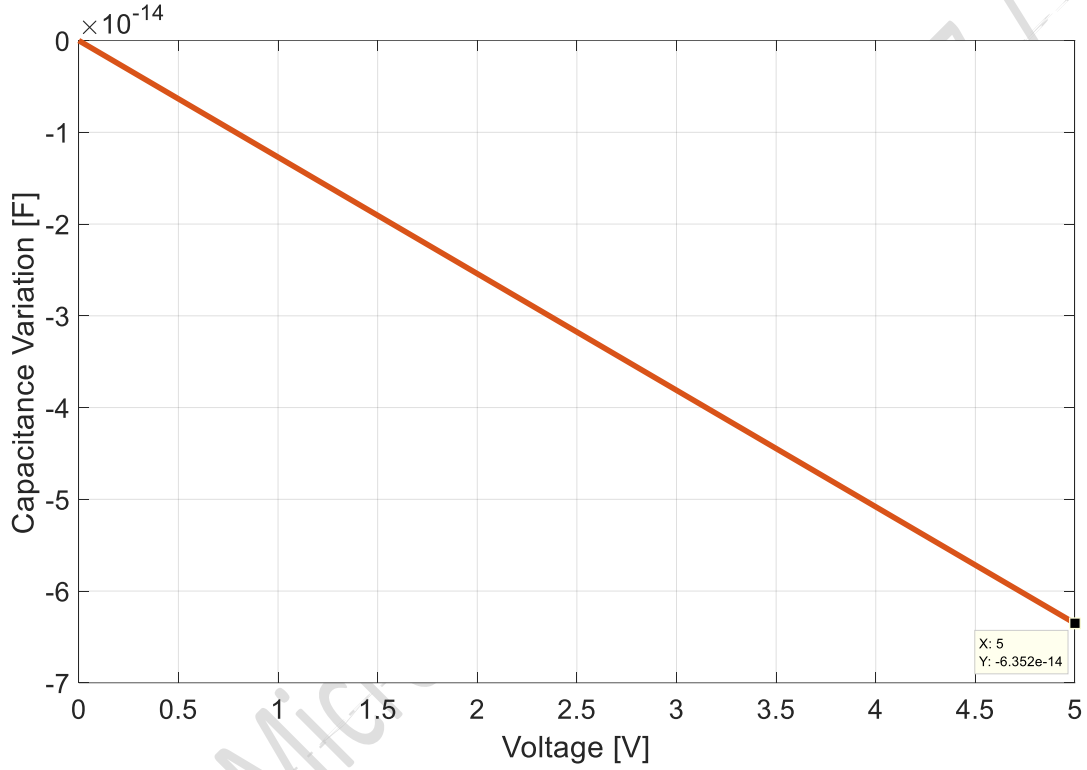

(iii)

The desired overall scale factor to cover a 3 V supply with a target FSR of 4 g units is:

$$SF = \frac{V_{DD}}{FSR} = \frac{3V}{4\,g} = 750\frac{mV}{g}$$

The expression of the scale factor can be written, for the given configuration, as the product of three terms : the gain from acceleration to displacement, the gain from displacement to capacitance variation (note the comb finger sensing) and the gain from capacitance to voltage change of the charge amplifier, followed by the second stage gain. Take care in accounting for the factor 9.8 if you want to express this in V/g.

$$SF = 2\frac{dx}{da}\frac{dC}{dx}\frac{dV}{dC}\,G_{eln}\cdot 9.8 = 2\frac{1}{\omega_0^2}\frac{2\epsilon_0 h\,(N_{L1}+N_{L2}+N_{L3})}{g}\frac{V_{DD}}{C_F}\,G_{eln}\cdot 9.8$$

By equating the two expressions of the SF, we find a needed electronic gain for the second stage G_{eln} = 6.67.

(iv)

In principle an increase of the bias voltage increases the sensitivity of a MEMS accelerometer, so we would easily answer that the new sensitivity is twice the value above, with the FSR that becomes halved to 2 g. In particular, in a comb-finger situation there is ideally no risk of pull-in.

However, in this situation we have ultra-narrow gaps and we are given the stiffness in the y direction. Note that, in the y-direction, the comb fingers resemble parallel plates, which may give rise to pull-in in the y-direction!

The calculation of the electrostatic stiffness in the y direction is (the first factor 2 is for the double facing of combs, the second factor 2 is for the symmetric structure):

$$k_{elec,y} = 2 \cdot \frac{2 \cdot C_{L1+L2+L3}}{g^2} V_{DD}^2 = 1835 \frac{N}{m}$$

This exceeds the mechanical stiffness in the y direction, thus causing pull-in and making the device not usable in this configuration. The electrostatic stiffness in the y-direction for the previous biasing configuration is instead of 459 N/m and thus causes no pull-in in the y-direction.

Finally, note that in all other point pull-in did not occur due to the lower (in modulus) equivalent stiffness, either due to the lower applied voltage (previous point) or due to the lower number of involved comb fingers (first two points).

Last Name Invacanza **Given Name** Allegra **ID Number** 20190719

Question n. 3

An imaging sensor is equipped with a specific mosaic of color filters (CFA), which features four different spectral bands. The positioning of the micro filters is shown in the zoomed image, and the right figure reports the spectral quantum efficiencies of the different channels. Other sensor parameters are given in the table.

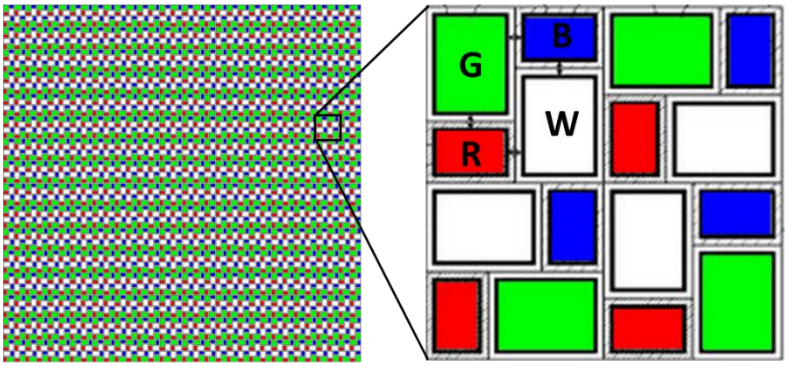

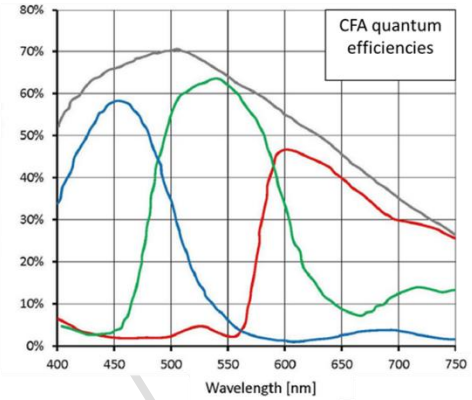

(i) at an intermediate wavelength in the visible range, find the F number ($F_\#$) for which diffraction and aberrations result in the same resolution. Is the pixel size well designed?

(ii) each photosite is implemented as a 4T topology pixel: comment on the value of the dark current shot noise, and calculate the required kTC noise rejection factor to have its contribution equal to the dark current shot noise at 3.5 ms integration;

(iii) calculate the conversion gain (in µV/e$^-$), the full well capacity (the maximum number of collectable electrons) and the DR of the different color channels;

Parameter	Symbol	Value
G/W pixel size	$l_{gw} \cdot w_{gw}$	6 µm·4 µm
R/B pixel size	$l_{rb} \cdot w_{rb}$	4 µm·2 µm
Dark current	i_d	0.05 fA
Pinned diode capacitance	C_{PPD}	3 fF
Floating diffusion capacitance	C_{FD}	0.05 fF
Gate capacitance	C_g	0.25 fF
Integration time	t_{int}	3.5 ms
Supply voltage	V_{DD}	5 V
ADC number of bits	N_{bit}	12
Aberration spot size	d_{Aber}	$3 \cdot 10^{-5}$ m/$F_\#$

(iv) which is the purpose of the W (monochrome) channel? Which system that you have studied resembles this configuration? Why, in your opinion, the area of green and monochrome channels is larger than for red and blue color channels? Why does the positioning of the color channels follow a 4x4 regular pattern instead of a 2x2 regular pattern?

Physical Constants

$\varepsilon_0 = 8.85\ 10^{-12}$ F/m
$k_B = 1.38\ 10^{-23}$ J/K
$q = 1.6\ 10^{-19}$ C
T = 300 K

(i)

The first asks to relate the sensor-limited resolution to the optics-limited resolution. The latter, in the end, is affected by both diffraction and aberration. We know how to express the diffraction spot size (Airy disk), and we are given an approximated formula for the aberrations (which, as expected, shows a spot decreasing with increasing $F_\#$). The F# at which the two contributions are matche dis readily obtained by equating:

$$\underbrace{2.44\,\lambda\,F_{\#}}_{diffraction} = \underbrace{\frac{30\mu m}{F_{\#}}}_{aberrations} \quad \rightarrow \quad F_{\#} = \sqrt{\frac{30\mu m}{2.44 \cdot 555\,nm}} = 4.7$$

With this value, the spot size caused by diffraction, as well as the circle of confusion caused by aberrations, are of:

$$d_{Airy} = d_{Aber} = 2.44\,\lambda\,F_{\#} = 6.4\,\mu m$$

The maximum dimension of a pixel is of $6\,\mu m$, which means that the sensor is well designed, in that the sensor resolution is well balanced with the optics resolution. Designing larger pixels would have worsened the resolution. Designing smaller pixels would have worsened the SNR due to the lower area.

Additionally (not requested), the graph aside shows graphically the two effects and, again, the solution of this question, with the two resolution curves crossing each other at a value $F_{\#}$ of about 4.7 for a 555-nm wavelength.

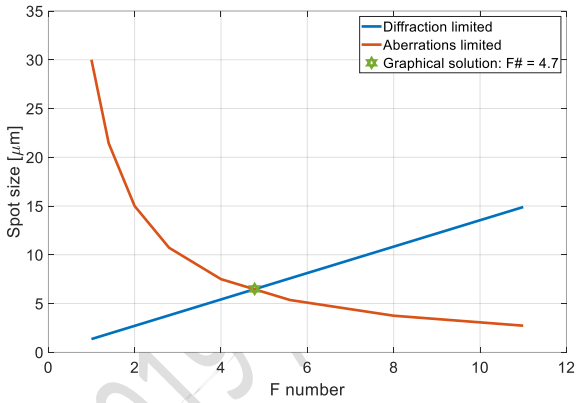

(ii)

As we are using a 4T topology with pinned photodiodes, the inhibition of surface-generated dark carriers lowers significantly the overall dark current. This is one of the well known advantages of a pinned photodiode.

The second advantage is the possibility to reject kTC noise (and part of the pixel offsets) by adopting correalted double sampling. This strategy does not cancel perfeclty kTC noise because of residual small differences in the two capacitances where the data before and after integration are stored. The effectiveness of kTC noise is usually characterized by the so called kTC noise rejection factor RF.

For this specific question, this can be found by equating the expression of kTC noise and of dark current shot noise, here written in terms of electrons rms:

$$\sigma_{d,shot,e} = \frac{\sqrt{q \cdot i_d \cdot t_{int}}}{q} = 1\,e^-_{rms}$$

$$\sigma_{kTC,e} = \frac{\sqrt{k_b T\left(C_{fd} + C_g\right)}}{q\,RF} = \sigma_{d,shot,e} = 1\,e^-_{rms}$$

Note that we have used only the capacitance of the floating diffusion and the capacitance of the source follower gate. Indeed, the pinned photodiode is decoupled from the floating diffusion node by the transfer gate. We thus find a required rejection factor value RF = 6.67.

(iii)

Even if the photosensing area is different for the three channels, in a pinned photodiode the sensing node is decoupled from the photodiode area. Therefore, the conversion gain, the full well capacity and the DR are identical for all the color channels of the proposed CFA :

$$CG = \frac{q}{C_g + C_{fd}} = 533 \frac{\mu V}{e^-}$$

$$FWC_e = \frac{V_{DD}}{CG} = 9375\ e^-$$

(note: the well capacity of the pinned photodiode itself is even larger, but the maximum readable value is calculated by taking into account the capacitance at which, in the end, the charge signal will be integrated). As we already have the full well charge in electrons, and as we already know kTC and dark shot noise in electrons rms, for the DR calculation we miss only the value of quantization noise, which can be calculated (in terms of electrons rms) as:

$$\sigma_{quant,e} = \frac{LSB_Q}{q\sqrt{12}} = \frac{LSB_V(C_g + C_{fd})}{q\sqrt{12}} = \frac{V_{DD}(C_g + C_{fd})}{2^{N_{bit}}\, q\sqrt{12}} = 0.66\ e^-_{rms}$$

We thus find the value of the DR, which exceeds 75 dB thanks to the 4T topology.

$$DR = 20\log_{10}\frac{FWC_e}{\sqrt{\left(\sigma_{quant,e} + \sigma_{kTC,e} + \sigma_{d,shot,e}\right)^2}} = 75\ dB$$

(iv)

This color filter array implements various differences with respect to the standard RGGB CFA (Bayer pattern). First, it shows 4 different spectral responses, where a monochrome (white) channe replaces one of the G channels. Second, it shows differences in the area of G/W channels with respect to B/G. Third, the positioning of the filters follows a 4x4 pattern instead of a 2x2 pattern.

The reasons why this topology is implemented can be motivated by the following considerations:

(a) the presence of 4 spectral channels resembles the operation of the human eye, when during daylight the cones are used to provide a faithful color response, while in dim light or dark only the rods are active to provide a satisfactory brightness image, through with poor color detection capability. The purpose of the W channel may thus be to capture good images (i.e. with good SNR) in the dark – though without giving a full-color output image. The W channel is indeed not filtered and lets most of impinging light pass towards Silicon for absorption and readout;

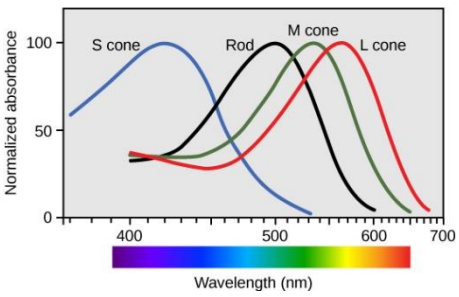

(b) the larger area of the G and W channels is probably due to the fact that these two channels have a response which is very similar to the overall photopic curve of the human eye. As the human eye resolution is more determined by the brightness channel than by the chrominance channels, it makes sense to try mimicking its behavior to deliver images which are as much faithful as possible to the human eye perception;

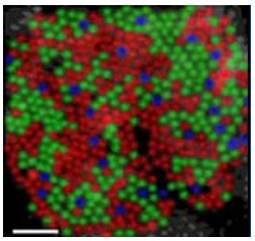

(c) the sparse configuration of the pixels aims at reducing chances of aliasing. Regular patterns, i.e. regular spatial sampling of the image, gives rise to possibilities of aliasing. This is avoided if – once more like in the human eye – a less predictable pattern is adopted.

Finally note that a larger area for the G/W channels enables to reduce the time at which the FWC (i.e. the maximum signal) is reached. As the maximum DR is obtained at short integration times, this has a positive effect on DR as well.